

Radiative lifetimes in Ti I

S. Salih* and J.E. Lawler

Department of Physics, University of Wisconsin, Madison, WI 53706, USA

Received March 22, accepted April 7, 1990

Abstract. Radiative lifetimes for more than 160 levels in Ti I are reported. These accurate lifetimes ($\pm 5\%$) are measured using time-resolved laser-induced fluorescence on a titanium atomic beam. These lifetimes confirm the recent renormalization of the Oxford Ti I oscillator strengths, confirm the revision of the solar abundance of titanium, and provide a foundation for a much more extensive set of Ti I oscillator strengths.

Key words: atomic and molecular data – sun: abundances

In a recent article in this journal, Grevesse et al. (1989) revised the absolute scale of the Oxford Ti I oscillator strengths and the solar abundance of titanium. These revisions were prompted by Rudolph and Helbig's (1982) measurement of 17 Ti I radiative lifetimes using time-resolved laser-induced fluorescence on a Ti atomic beam. Time-resolved laser-induced fluorescence on slow atomic and ionic beams is recognized as the most broadly applicable and accurate method for measuring radiative lifetimes (Lawler, 1987). The goals of this work are: (1) to test and if possible confirm the work by Rudolph and Helbig, and (2) to lay the foundation for a much more comprehensive set of Ti I oscillator strengths. It would be quite valuable for synthesizing stellar spectra to determine ($\pm 10\%$) the oscillator strength of all classified lines of Ti I and ultimately other iron group spectra.

Although Grevesse et al. used radiative lifetimes to normalize relative absorption oscillator strengths, it is more common to use lifetimes to normalize relative emission line strengths or branching fractions. The application of powerful Fourier transform spectrometers (FTS) such as the 1.0 m FTS at the U. S. National Solar Observatory (Brault, 1976) in determining emission branching fractions has greatly improved the quality and quantity of available data. It is desirable to have a large set of accurate lifetimes for levels spread over a wide range of excitation energy. If a hollow cathode discharge is used as the emission source for the measurement of branching fractions, then it is necessary to have a lifetime for each upper level. Hollow cathode discharges produce atomic level populations far from Boltzmann equilibrium due to the low collision rates. They produce sharp emission lines for the same reason.

Recently Whaling and Brault (1988) have shown that Inductively Coupled Plasma (ICP) sources produce level popula-

tions which are close to Boltzmann equilibrium. If an extensive set of accurate lifetimes for levels distributed over a wide energy range is available, then it may be possible to interpolate on a Boltzmann plot and determine populations of levels for which lifetimes have not yet been measured. Such schemes have the potential for determining ($\pm 10\%$) oscillator strengths for all classified lines in a spectrum.

We report accurate radiative lifetimes for more than 160 Ti I levels with excitation energies ranging from $19,000\text{ cm}^{-1}$ to $48,000\text{ cm}^{-1}$. Figure 1 is a schematic of the experiment. The apparatus is an improved version of that used by Duquette et al. (1981) to produce atomic beams. The fact that the source has produced an atomic and/or ionic beam of 25 different elements is an indication of its versatility and reliability. The beam source is based on a low-pressure large-bore hollow cathode discharge. The hollow cathode is used as a beam source by sealing one end of the cathode except for a 1.0 mm diameter opening. The opening is flared outward at an angle of 45° to serve as a nozzle for forming an uncollimated atomic or ionic beam. The hollow cathode and the scattering chamber are at ground potential. Argon, the sputtering gas, flows continuously into the hollow cathode discharge. A 10 cm diffusion pump evacuates the scattering chamber. The scattering chamber is sealed from the discharge, except for the nozzle, and is maintained at a much lower pressure than the discharge. The argon pressure in the discharge is typically 0.3 Torr, and the pressure in the scattering chamber is approximately 10^{-4} Torr.

The discharge current is operated as high as 200 mA dc or as high as 30 A in a $5\text{ }\mu\text{s}$ pulse. One of the key advantages of the atomic/ionic beam source is that it produces both atoms and ions in high lying metastable levels. The large pulsed currents further enhance this advantage. The large populations in all metastable levels provide great flexibility in the choice of lower level for laser excitation. Recently we have learned that low lying odd parity levels with long ($\geq 10^{-4}$ s) radiative lifetimes also have useful populations in the atomic beam. This discovery enabled us to excite high lying even parity Ti I level with a single dye laser instead of two dye lasers (Marsden et al., 1988).

The atomic beam is crossed by a N_2 laser pumped dye laser beam 1 cm from the nozzle. The dye laser produces a pulse of 3 ns duration (FWHM) with a 0.2 cm^{-1} bandwidth and a peak power of up to 40 kW. A set of KDP (potassium dihydrogen phosphate) and BBO (Beta Barium Borate) crystal frequency doublers extends the tuning range of the dye laser to 205 nm in the ultraviolet. The fluorescence is detected along an axis orthogonal to both the atomic beam and laser beam. In order to minimize scattered light, several sets of light baffles are arranged along the laser beam axis

Send offprint requests to: J.E. Lawler

*Present address: Physics Department, AN-Najah University, Nablus – West Bank via Israel

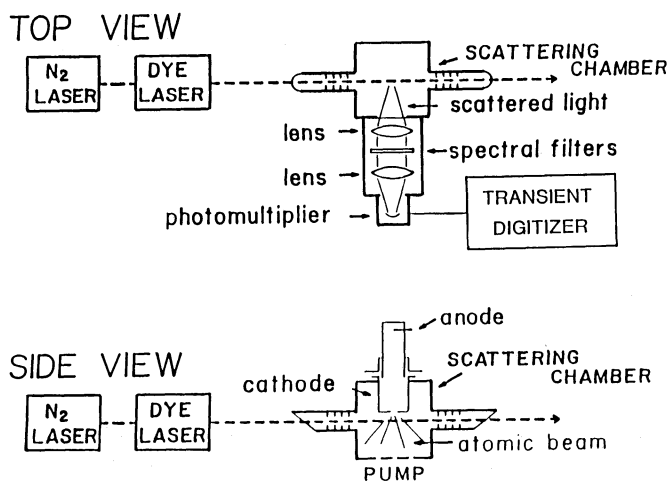


Fig. 1. Schematic of the experimental apparatus

inside and outside the Brewster windows that pass the laser beam into and out of the scattering chamber.

The lifetime experiment has a dynamic range from 2 ns to 2 μ s. The finite electronic bandwidth of the detection apparatus is a concern at the 2 nsec end of the range. The base of the 1P28A photomultiplier is wired for very low overall inductance in order to maintain the full electronic bandwidth of the tube. The base includes bypass capacitors in order to provide good linearity to 10 mA of peak anode current, and includes small damping resistors in order to reduce ringing (Harris et al., 1976). The signal from the photomultiplier is logged using either a Tektronix 7912AD transient digitizer or a Princeton Applied Research 162-163-165 boxcar averager. Only the digitizer is shown in Fig. 1. The vast majority of the \sim 4500 fluorescence decay curves were recorded using the transient digitizer, because the digitizer has a data collection rate which is two orders of magnitude larger than that of the boxcar. Some lifetimes were measured using both systems in order to check for systematic differences. Both data logging systems are capable of measuring lifetimes as short as

Table 1. Radiative lifetimes of odd parity Ti I levels

Configuration	Term	J	Level (cm^{-1})	Laser wavelength in air (nm)	Lifetime (ns) $\pm 5\%$ or ± 0.2 ns
$3d^2(^3F)3s4p(^3P^o)$	z^3F^o	2	19 322.988	517.38, 521.97	184
		3	19 421.576	514.75, 519.30, 525.21	191
		4	19 573.968	515.22, 521.04	195
$3d^2(^3F)4s4p(^3P^o)$	z^3D^o	1	19 937.859	501.42	159
		2	20 006.032	499.71, 504.00	168
		3	20 126.055	500.97, 506.47	178
$3d^2(^3F)4s4p(^3P^o)$	z^3G^o	3	21 469.494	465.65, 469.37	305
		4	21 588.496	466.76, 471.53	290
		5	21 739.713	468.19	278
$3d^2(^3P)4s4p(^3P^o)$	z^5S^o	2	25 102.88	398.25, 400.97	116
$3d^2(^3F)4s4p(^1P^o)$	y^3F^o	2	25 107.417	400.89, 538.92	17.7
		3	25 227.217	398.98, 536.66	16.9
		4	25 388.334	396.43, 399.86	18.3
$3d^3(^4F)4p$	y^3D^o	1	25 317.813	394.87, 592.21	14.5
$3d^2(^1D)4s4p(^3P^o)$		2	25 438.898	395.63, 589.93	18.4
$3d^2(^1D)4s4p(^3P^o)$		z^3P^o	2	25 493.722	392.14, 394.78
$3d^2(^3P)4s4p(^3P^o)$	y^5D^o	3	25 797.60	390.10, 393.42	340
		4	25 926.771	391.43, 523.86	258
$3d^2(^3P)4s4p(^3P^o)$	y^5G^o	3	25 643.695	543.67, 586.65	14.6
$3d^3(^4F)4p$		2	26 494.322	501.42, 502.48	13.4
		3	26 564.385	500.72, 502.29	13.3
		4	26 657.409	499.95, 502.00	13.1
5		26 772.965	499.11, 501.62	13.0	
6	26 910.705	498.17	12.9		
$3d^2(^1D)4s4p(^3P^o)$	x^3F^o	2	26 803.417	372.98, 493.77	15.9
		3	26 892.926	377.17, 492.62	15.8
		4	27 025.652	375.29, 655.61	15.4
$3d^2(^1D)4s4p(^3P^o)$	x^3D^o	1	27 355.042	365.46, 528.44	81.0
		2	27 418.015	366.90, 528.24	89.0
		3	27 480.047	368.99, 529.58	91.0
$3d^2(^3F)4s4p(^1P^o)$	y^3G^o	3	27 498.975	363.55, 626.11	9.3
		4	27 614.667	364.27, 625.81	9.5
		5	27 750.124	365.35, 478.17, 625.87	10.3
$3d^2(^3P)4s4p(^3P^o)$	z^5P^o	3	27 887.74	363.52	360
$3d^2(^1D)4s4p(^1P^o)$	y^1D^o	2	27 907.026	484.09	44.9

Table 1 (continued)

Configuration	Term	<i>J</i>	Level (cm ⁻¹)	Laser wavelength in air (nm)	Lifetime (ns) ± 5% or ± 0.2 ns	
$3d^3(^4F)4p$	y^5F^o	1	28 596.293	453.61, 454.47	8.9	
		2	28 638.832	452.73, 454.88	8.9	
		3	28 702.768	453.56, 455.25	8.7	
		4	28 788.372	453.48, 455.55	8.7	
		5	28 896.062	451.27, 453.32	8.7	
$3d^2(^3F)4s4p(^1P^o)$	w^3D^o	1	29 661.232	472.26, 551.44	9.4	
		2	29 768.655	548.19, 551.45	9.1	
$3d^3(^4F)4p$	x^5D^o	0	29 829.097	429.58	7.2	
		1	29 855.248	429.09, 429.87	7.1	
		2	29 907.273	430.06, 547.27	7.2	
		3	29 986.185	430.11, 549.02	7.4	
		4	30 060.328	428.74, 430.59	7.1	
$3d^3(^4F)4p$	x^3G^o	3	29 912.262	547.12, 551.25	8.6	
$3d^2(^1G)4s4p(^3P^o)$		3	29 914.720	431.44, 469.08	10.5	
		4	29 971.078	545.37	10.7	
		5	30 039.211	547.42	10.7	
$3d^2(^3P)4s4p(^3P^o)$	v^3D^o	1	31 184.021	320.58, 508.71	51.9	
		2	31 190.631	322.27, 511.34	49.5	
		3	31 205.985	324.38, 442.28, 514.55	49.0	
$3d^3(^4F)4p$	w^3G^o	3	31 373.801	503.84, 506.60	6.5	
		4	31 489.451	503.65, 507.15	6.3	
		5	31 628.668	319.99, 503.59	6.1	
		$3d^2(^1D)4s4p(^1P^o)$	3	32 857.721	390.48, 482.04	8.8
		$3d^3(^4F)4p$	x^3P^o	0	33 085.153	406.51
$3d^3(^4F)4p$	w^3F^o	1	33 090.492	406.42, 408.25	13.2	
		2	33 114.412	406.03, 407.85	13.3	
		2	33 655.853	297.04, 451.87	50.7	
		3	33 680.130	298.33, 539.71	47.5	
		4	33 700.874	300.09, 540.96	45.4	
$3d^2(^1D)4s4p(^1P^o)$	z^1P^o	1	33 660.671	378.60	9.5	
$3d^2(^1G)4s4p(^3P^o)$	v^3F^o	2	33 980.639	445.33, 529.73	4.8	
		3	34 078.580	445.53, 528.35	4.8	
		4	34 204.971	445.74, 526.60	4.9	
		5	34 700.212	442.71, 609.12	14.3	
$3d^2(^3P)4s4p(^3P^o)$	y^1P^o	1	34 947.120	361.02, 379.47	19.9	
$3d^2(^3P)4s4p(^3P^o)$	x^1D^o	2	35 035.147	376.65	25.7	
$3d^3(^2G)4p$	y^3S^o	1	35 439.228	370.23, 371.00	6.9	
		4	35 454.051	491.36, 574.00	16.9	
		5	35 559.627	489.99, 573.95	16.8	
		6	35 685.160	488.51, 571.51	16.7	
		$3d^3(^4P)4p$	w^5D^o	0	35 503.40	464.52
		1	35 527.76	464.00, 465.00	10.4	
		2	35 577.14	282.35, 462.93, 463.94	10.4	
		3	35 652.95	462.31, 463.97	10.3	
		4	35 757.51	461.73	10.3	
$3d^2(^1G)4s4p(^1P^o)$	y^1G^o	4	36 000.144	418.61, 556.55, 564.41	14.0	
$3d^3(^4P)4p$	y^5P^o	1	36 298.43	447.97, 448.91	9.0	
		2	36 340.67	447.12, 449.62	9.1	
		3	36 414.58	446.58, 448.13	9.0	
$3d^3(^a^2D)4p$	w^3P^o	1	37 172.947	268.93, 506.21	9.5	
		2	37 325.407	269.06, 505.29, 542.92	9.4	
$3d^3(^4P)4p$	y^5S^o	2	37 359.13	268.82, 428.50, 504.43	8.1	
$3d^3(^2G)4p$	v^3G^o	3	37 555.021	266.20, 445.37	9.7	
		4	37 617.868	266.96, 445.09	8.8	
		5	37 690.320	267.99, 444.92	8.7	

Table 1 (continued)

Configuration	Term	<i>J</i>	Level (cm ⁻¹)	Laser wavelength in air (nm)	Lifetime (ns) ± 5% or ± 0.2 ns
<i>3d4s²4p</i>	<i>x¹F^o</i>	3	37 622.573	265.72, 444.04	11.1
<i>3d³(<i>a</i>²<i>D</i>)4p</i>	<i>u³F^o</i>	2	37 654.77	265.49	13.9
		3	37 743.933	266.06, 442.61, 491.99	13.2
		4	37 852.434	265.30, 441.73, 492.18	12.9
		4	37 852.21	264.11, 379.83	4.0
<i>3d²(³<i>P</i>)4s4p(¹<i>P^o</i>)</i>	<i>u³D^o</i>	1	37 852.21	264.11, 379.83	4.0
		2	37 976.78	264.43, 379.59	4.0
		3	38 159.71	264.66, 378.93, 484.84	4.1
<i>3d³(²<i>G</i>)4p</i>	<i>t³F^o</i>	2	38 451.298	259.99, 428.27	5.9
		3	38 544.38	260.52, 261.99	5.9
		4	38 670.710	261.13, 426.31	5.9
<i>3d³(²<i>H</i>)4p</i>	<i>z³F^o</i>	5	38 572.692	486.83	16.2
		6	38 668.832	487.01	16.1
		7	38 779.856	485.60	15.9
		1	38 654.23	368.60, 469.69	6.2
<i>3d³(²<i>P</i>)4p</i>	<i>t³D^o</i>	2	38 699.767	369.45, 468.69	6.1
		3	38 764.832	259.03, 370.43	6.0
		4	38 959.499	477.83, 550.39	7.3
<i>3d³(²<i>G</i>)4p</i>	<i>x¹G^o</i>	4	38 959.499	477.83, 550.39	7.3
<i>3d³(<i>a</i>²<i>D</i>)4p</i>	<i>x¹P^o</i>	1	39 077.713	314.15, 529.84	9.2
<i>3d³(²<i>H</i>)4p</i>	<i>x³H^o</i>	4	39 115.958	474.28, 479.98	10.3
		5	39 152.057	416.63, 475.81	10.2
		6	39 198.320	416.94, 475.93	10.3
		2	39 265.80	255.71, 312.31	11.5
<i>3d³(²<i>P</i>)4p</i>	<i>w¹D^o</i>	2	39 265.80	255.71, 312.31	11.5
<i>3d³(<i>a</i>²<i>D</i>)4p</i>	<i>s³D^o</i>	1	39 662.15	252.05	8.2
		2	39 686.10	251.90, 479.25	8.1
		3	39 715.437	254.19, 480.54	8.0
<i>3d³(<i>a</i>²<i>D</i>)4p</i>	<i>w¹F^o</i>	3	40 302.950	302.51, 497.53	11.2
<i>3d³(²<i>H</i>)4p</i>	<i>z¹I^o</i>	6	40 319.80	512.04	16.9
<i>3d³(⁴<i>P</i>)4p</i>	<i>r³D^o</i>	1	40 556.07	246.50, 311.25	8.2
		2	40 670.60	245.80, 310.68	8.2
		3	40 844.19	245.78, 247.10	8.1
<i>3d³(²<i>P</i>)4p</i>	<i>x³S^o</i>	1	40 844.19	308.48, 309.01	7.2
<i>3d³(²<i>H</i>)4p</i>	<i>y¹H^o</i>	5	41 039.874	245.91, 439.39, 493.83	11.8
<i>3d²4s(⁴<i>F</i>)5p?</i>	<i>u³G^o</i>	3	41 170.003	242.82, 432.17	11.5
		4	41 255.400	243.32, 432.51	12.2
		5	41 341.553	244.10, 431.86	11.9
		2	41 337.43	241.84, 417.10	16.3
<i>3d4s²4p</i>	<i>s³F^o</i>	3	41 457.653	242.13, 243.41	15.3
		4	41 624.209	241.16, 242.42	16.4
		3	41 585.24	291.21	3.8
<i>3d4s²4p</i>	<i>q³D^o</i>	1	42 146.39	237.20, 296.57, 297.06	7.8
		2	42 206.88	237.81, 296.52, 297.49	8.1
		3	42 311.269	296.57, 403.58	8.1
<i>3d²4s(⁴<i>F</i>)5p?</i>	<i>p³D^o</i>	1	42 194.04	236.93, 296.14, 296.64	29.9
		2	42 269.78	237.46, 280.75, 295.97	24.0
		3	42 376.45	238.08, 280.55, 296.00	23.6
		1	42 927.55	280.25, 437.24	4.0
<i>3d³(²<i>F</i>)4p</i>	<i>w¹P^o</i>	4	43 674.130	436.97	11.5
		2	43 710.28	274.23	3.4
		2	43 799.455	273.56	7.7
<i>3d³(<i>a</i>²<i>D</i>)4p</i>	<i>u¹D^o</i>	2	43 799.455	273.56	7.7
<i>3d²(¹<i>G</i>)4s4p(¹<i>P^o</i>)</i>	<i>x¹H^o</i>	5	44 163.24	311.97, 427.82	4.7
<i>3d³(⁴<i>P</i>)4p</i>	<i>w³S^o</i>	1	44 858.03	274.91, 275.74	4.0
		0	45 040.70	273.53	3.0
		1	45 090.73	272.74, 273.98	3.0
		2	45 178.06	272.51, 273.33	3.0
<i>3d²4s(²<i>F</i>)5p</i>	<i>u¹G^o</i>	4	46 257.67	292.83, 392.63	3.0
<i>3d³(²<i>F</i>)4p</i>	<i>u¹F^o</i>	3	48 365.09	243.18, 275.81	3.4

Table 2. Radiative lifetimes of even parity Ti I levels

Configuration	Terms	<i>J</i>	Level (cm^{-1})	Laser wavelength in air (nm)	Lifetimes (nsec) $\pm 5\%$ or ± 0.2 ns
$3d^24s(^4F)5s$	e^5F	2	36 013.57	496.48, 498.92	9.9
		3	36 096.47	496.86, 500.10	10.0
		4	36 208.92	497.31, 501.33	10.0
		5	36 351.43	502.56	9.9
$3d^24s(^4F)4d$	e^5G	4	41 818.70	386.84	6.7
		6	42 019.22	388.22, 391.12	6.8
$3d^24s(^4F)4d$	e^5H	4	41 917.05	385.37, 387.32	7.4
		5	42 018.01	385.81, 388.23	6.7
		6	42 123.77	386.64, 389.53	6.7
		7	42 205.59	388.29	6.6
$3d^24p^2$	g^5G	2	46 943.91	321.79	4.0
		3	47 030.28	321.92	4.6
		4	47 139.86	322.14	3.8
		5	47 280.69	322.35	3.7
		6	47 446.84	322.61	3.8

Table 3. Comparison of laser-induced fluorescence lifetime measurements

Level (cm^{-1})	Designation	Lifetime (ns)	
		Rudolph and Helbig	This work
19937.859	$z^3D_1^o$	165(12)	159(8)
21469.494	$z^3G_3^o$	371(26)	305(15)
21588.496	$z^3G_4^o$	310(22)	290(15)
21739.713	$z^3G_5^o$	328(23)	278(14)
25107.417	$y^3F_2^o$	17.7(12)	17.7(9)
25227.217	$y^3F_3^o$	16.8(12)	16.9(8)
25388.334	$y^3F_4^o$	18.8(13)	18.3(9)
25317.813	$y^3D_1^o$	15.5(11)	14.5(7)
25438.898	$J=2$	18.4(13)	18.4(9)
25643.695	$J=3$	15.0(11)	14.6(7)
25493.722	$z^3P_2^o$	54.0(38)	58.0(29)
26803.417	$x^3F_2^o$	15.6(11)	15.9(8)
26892.926	$x^3F_3^o$	16.2(11)	15.8(8)
27025.652	$x^3F_4^o$	15.5(11)	15.4(8)
27498.975	$y^3G_3^o$	9.6(7)	9.3(5)
27614.667	$y^3G_4^o$	10.0(7)	9.5(5)
27750.124	$y^3G_5^o$	10.6(7)	10.3(5)

2 ns. The boxcar has a minimum window width of 75 ps. The transient digitizer has an analog bandwidth of 500 MHz and a sampling rate as high as 100 GHz. The most convincing test of the electronic bandwidth of the detection system involves measuring the short and very well known He 3^1P^o and 4^1P^o lifetimes (Salih et al., 1985).

Optimum fluorescence collection efficiency for short lived levels is achieved by imaging the intersection of the laser and atomic beams onto the photomultiplier cathode. Two lenses

comprising an $f/1$ system with unity magnification are used. The fluorescence light is roughly collimated between the two lenses. There is a provision for inserting interference filters and/or dye filters between the lenses. Occasionally branching ratios are favorable for observing fluorescence at a wavelength much different than the laser wavelength. Filters are used to block all scattered laser light and isolate the laser-induced fluorescence whenever possible. Repopulation by radiative cascades from higher lying levels is not a problem because of the highly selective laser excitation. Filters are used to block emission from lower lying levels which are populated by radiative cascade.

The imaging of the intersection of the laser and atomic beams directly onto the photomultiplier cathode is not optimum for long lived levels ($\sim 1 \mu\text{s}$). Unfortunately this arrangement can lead to systematic error in long lifetimes caused by atomic motion. The image of the radiating atoms moves across the photocathode which has a position dependent response. In addition, the efficiency of the fluorescence collection system is weakly position dependent. This systematic error is said to be due to atoms escaping from the observation region before radiating. This systematic error has been studied in detail previously, and techniques for eliminating the error have been developed (Marsden et al., 1988). No lifetimes in the microsecond range were measured in this Ti I work, and thus systematic error due to atoms escaping from the observation region before radiating was not a problem.

Other possible systematic errors from radiation trapping, collisional quenching, or Zeeman quantum beats are unimportant. Tests for radiation trapping are routinely performed by varying the atomic beam intensity. Many such tests on strong resonance transitions have been performed and radiation trapping of metal atom transitions has not been detectable. Collisional quenching is not a problem because of the low scattering chamber pressure, 10^{-4} Torr of Ar. The absence of collisional quenching is confirmed by varying the scattering chamber pressure when measuring long lifetimes. Zeeman quantum beats are avoided by measuring short (< 300 ns) lifetimes in zero magnetic

field (< 20 mGauss) and by measuring long (> 300 ns) lifetimes in a high (30 Gauss) field. We quote a total uncertainty which is the greater of $\pm 5\%$ or ± 0.2 nsec on our lifetime measurements. This uncertainty includes both systematic and random error.

The total uncertainty which is the greater of $\pm 5\%$ or ± 0.2 ns applies to both odd and even parity levels. The selective laser excitation of atoms in a beam environment produces lifetimes for odd and even parity levels which are essentially free from systematic error. The high lying even parity levels do have somewhat greater likelihood of producing detectable fluorescence from lower lying odd parity levels populated by radiative cascade. This error is avoided by using narrow band interference and/or dye filters in the fluorescence collection system.

Our lifetime measurements on odd parity levels are summarized in Table 1 and even parity levels are summarized in Table 2. The configuration and term assignments as well as the level energies are from Sugar and Corliss (1985). Most levels have more than one laser wavelength listed. The wavelengths, which have been rounded to 0.01 nm, are from Russell (1927) or from Wilson and Thekaekara (1961). It is desirable, when possible, to use more than one transition for laser excitation. This provides a check that the transition has been correctly classified, is correctly identified in the experiment, and is unblended. We learned from additional tests with fluorescence filters that the 551.18 nm line of Ti I is misclassified. The upper level of this line was previously identified as the $z^1S_0^o$ level at $38,200.94 \text{ cm}^{-1}$ (Russell, 1927). We do not believe that the $z^1S_0^o$ level exists. The lifetime of 10.7(5) ns and the observation of strong UV fluorescence from laser excitation at 551.18 nm indicate that the correct upper level is probably the $x^3G_3^o$ level at $29914.720 \text{ cm}^{-1}$.

Essentially all of the work on Ti I transition probabilities by many different authors has recently been compiled, in some cases adjusted, and evaluated for accuracy by Martin et al. (1988). We will restrict our comparisons in this paper to other direct lifetime measurements using laser-induced fluorescence. Table 3 compares measurements by Rudolph and Helbig (1982), which were used to renormalize the Oxford Ti I oscillator strengths, to our measurements. The agreement, except for the z^3G levels, is excellent. The average difference for all 17 levels between Rudolph and Helbig's lifetimes and ours is $+4.0\%$ and the RMS difference 7.7%. A subset of 9 lifetimes was used to renormalize the Oxford Ti I oscillator strengths. The average difference for these 9 levels between Rudolph and Helbig's lifetimes and ours is $+2.6\%$ and

the RMS difference is 3.5%. Agreement between different laser experiments to better than 5% is actually routine. This level of agreement confirms the renormalization of the Oxford Ti I oscillator strengths.

In summary, we report radiative lifetimes for more than 160 Ti I levels. These lifetimes are measured using time-resolved laser-induced fluorescence. Our measurements confirm the renormalization of the Oxford Ti I oscillator strengths proposed by Grevesse et al. on the basis of lifetime measurements by Rudolph and Helbig. More importantly our measurements lay the foundation for determining an accurate transition probability for essentially every classified Ti I line using FTS data.

Acknowledgements. This research is supported by the U.S. National Science Foundation under Grant AST 88-21051. T. O'Brian, M. Wickliffe, and J.E. Lawler discovered, during recent work on Fe I, that long lived odd parity levels are populated in the beam. The discovery made it possible to excite high lying even parity levels with a single laser pulse. The Fe I work is in collaboration with W. Whaling and J. Brault.

References

- Brault, J.W.: 1976, *J. Opt. Soc. Am.* **66**, 1081
 Duquette, D.W., Salih, S., Lawler, J.E.: 1981, *Phys. Letters* **83A**, 214
 Grevesse, N., Blackwell, D.E., Petford, A.D.: 1989, *Astron. Astrophys.* **208**, 157
 Harris, J.M., Lytle, F.E., McCain, T.C.: 1976, *Ana. Chem.* **48**, 2095
 Lawler, J.E.: 1987, in *Lasers, Spectroscopy, and New Ideas*, eds. W.M. Yen, M.D. Levenson, Springer Series in Optical Sciences **54**, 125
 Marsden, G.C., Den Hartog, E.A., Lawler, J.E., Dakin, J.T., Roberts, V.D.: 1988, *J. Opt. Soc. Am. B* **5**, 606
 Martin, G.A., Fuhr, J.R., Wiese, W.L.: 1988, *J. Phys. Chem. Ref. Data* **17**, Suppl. 3
 Rudolph, J., Helbig, V.: 1982, *Phys. B: At. Mol. Phys.* **15**, L599
 Russell, H.N.: 1927, *Astrophys. J.* **66**, 347
 Salih, S., Lawler, J.E., Whaling, W.: 1985, *Phys. Rev.* **A31**, 744
 Sugar, J., Corliss C.: 1985, *J. Phys. Chem. Ref. Data* **14**, Suppl. 2
 Whaling, W., Brault J.W.: 1988, *Phys. Scripta* **38**, 707
 Wilson, C.M., Thekaekara, M.P.: *J. Opt. Soc. Am.* **51**, 289